RSC Advances

ROYAL SOCIETY OF CHEMISTRY

www.rsc.org/advances

TiO_2 nanoparticals/ZnO nanowires hybrid photoanode for enhanced quantum dots-sensitized solar cell performance

Jianping Deng, Minqiang Wang*, Chengao Yang, Jing Liu, Xiaohui Song

Electronic Materials Research Laboratory (EMRL), Key Laboratory of Education Ministry; International Center for Dielectric Research, Xi'an Jiaotong University, Xi'an, 710049, China.

Fax: +86-29-82668794; Tel: +86-29-82668794.

E-mail: mqwang@mail.xjtu.edu.cn

Abstract

A hybrid structured TiO_2/ZnO photoanode composed of highly ordered ZnO nanowires (NWs) and small TiO_2 nanoparticals (NPs) filling in the gap among ZnO NWs. In this way, ZnO NWs provide a direct pathway to facilitate electron collection and transport, and increase light scattering and trapping. TiO_2 NPs provide a large specific surface to effectively adsorb quantum dots (QDs). In experiment, the density of ZnO NW arrays was first controlled by regulating the ratio of TiO_2 NPs to ZnO NPs and the concentration of ZnO NPs in the hybrid NPs seeds precursor, and then the TiO_2 paste was successfully filled in the gap among NWs by a large centrifugal force. Using TiO_2 NP/ZnO NW films as photoanodes, we fabricated CdSe QDs sensitized solar cells and tested their photovoltaic (PV) performances. The results exhibited a remarkably enhanced short-circuit current density (Jsc) of 7.9 mA/cm^2 and power conversion efficiency (η) of 1.55%, this η has a 19.2% and 30.3% enhancements as compared to the TiO_2 NPs device with η of 1.3% and ZnO NWs device with η of 1.19%.

Key words

ZnO nanowires; porous TiO_2; quantum dots; solar cells

Introduction

In recent years, photoelectrochemical (PEC) cells have attracted worldwide attention as cheap alternatives to conventional devices for solar energy conversion. Generally speaking, a sequence of physical processes in PEC cells include: i) the incident photons are captured, electron–hole pairs are generated, ii) the electrons and holes separate quickly into respective transfer material, and iii) the carriers are transported to opposing electrodes. The QDs-sensitized solar cell (QDSSCs) is one of PEC cells. In order to improve efficiency of QDSSCs, much effort has been made. Apart from the search for lower band gap QDs (PbSe, PbTe) [1, 2], electrolyte [3] and counter electrode [4], a large number of research studies focused on nanostructured photoanodes [5, 6]. We have reported a novel structure (subsectionally sensitized cells using a double-layer ZnO nanorods) [7]. Conventional QDSSCs are fabricated using porous NP films. The NP films provide the very high surface areas to ensure sufficient sensitizer loading. However, the major drawback of the NP films is high charge recombination loss due to the electron trapping and scattering at grain boundary and inefficient light scattering ability within small-sized NPs (10–20 nm) in the disordered network [5, 8]. To overcome this obstacle, 1D nanostructure has been widely investigated as photoelectrodes for solar energy conversion devices. They can offer a continuous pathway for photogenerated electrons to transport along the long axis of 1D and a large decrease of grain boundaries as well as affording low reflectance owing to light scattering and trapping. Besides, the electron diffusion coefficient in single crystalline is more than 2 orders of magnitude higher than that in 0D NPs [9]. Despite of the advantageous characteristics noted above, the efficiency of QDSSCs using the 1D nanostructured photoanode remains low because the specific surface area of 1D nanostructure films is roughly an order of magnitude lower than that of NP films. There is considerable free space between adjacent 1D nanostructure, which results in limited sensitizer loading [10, 11].

Herein, we reported a hybrid structured TiO_2/ZnO photoanode composed of a highly ordered ZnO NWs and small TiO_2 NPs filling in the gap among ZnO NWs. This

hybrid structure not only keeps high surface areas of NPs films but also maintains the advantage of 1D nanostructure, including the light scattering and trapping and the higher electron diffusion coefficient. In this structure, TiO_2 NPs can effectively adsorb QDs, and ZnO NWs act as highway which breadthwise receive photogenerated electrons and reduce the interface resistance of NPs, and then rapidly transport the electron to indium tin oxides (ITO) substrate. In this paper the commercial P_{25} powder is used owing to low cost and unique physical characteristics, ZnO NWs are used due to their well-developed synthetic methods and excellent electrical properties [12]. The resulting hybrid structured films were subsequently exploited as photoanodes in QDSSCs, exhibiting a markedly enhanced short-circuit current density (Jsc) of 7.9 mA/cm^2 and power conversion efficiency (η) of 1.55%, this η has a 19.2% and 30.3% enhancements as compared to the TiO_2 NPs device with η of 1.3% and ZnO NWs device with η of 1.19%, which can be attributed primarily to the synergistic effect of higher sensitized loading due to the presence of large surface area, superior light scattering ability and trapping, and higher electron diffusion coefficient .

Experimental section

Preparation of TiO_2 sol and TiO_2 NPs/ZnO NPs hybrid colloids

Preparation of TiO_2 sol. 3.4ml of Tetra-n-butyl Titanate was added into 8.3ml of dieth -anolamine, the mixture of 1.8ml of deionized water and 100ml of ethanol was then added. After stirring for 1h, the mixture was aged for 24h at 30°C.

Preparation of TiO_2 NPs/ZnO NPs hybrid colloids. 1.64g of zinc acetate and 0.96g of KOH were dissolved in 84ml and 46ml of methanol, respectively. Then KOH solution was added into zinc acetate solution in a flask equipped at room temperature. The system reacted under constant stirring for 2h at 60°C. The obtained QDs were separated by centrifugation, washed thoroughly by methanol and dispersed in methanol (50mg/ml).

Added 3.6ml of Tetra-n-butyl Titanate into 7.2ml of ethanol, then added 7.2ml of acetic acid glacial and 18ml of deionized water successively. After stirring for 1h, the

mixture reacted in the sealed container for 12h at 200°C. As ZnO NPs, Galactoid TiO_2 NPs were separated, washed and then dispersed (50mg/ml).

0.9, 0.5 and 0.1ml of as-prepared 50mg/ml ZnO NPs colloids were diluted using 1ml of methanol, respectively, and then 0.1, 0.5 and 0.9ml of as-prepared 50 mg/ml TiO_2 NPs colloid were added into 1.9, 1.5 and 1.1ml of diluted ZnO NPs colloid, respectively. The ratio of ZnO to TiO_2 were 22.5:2.5, 11.5:11.5 and 2.5:22.5 (mg/ml: mg/ml), by which the effect of the ratio on the density of ZnO NWs was investigated. For investigating the effect of concentration of ZnO NPs on ZnO NWs, we diluted the hybrid colloid to 0.625, 0.156 and 0.039mg/ml under the best ratio (2.5:22.5), respectively.

Preparation of hybrid photoelectrods

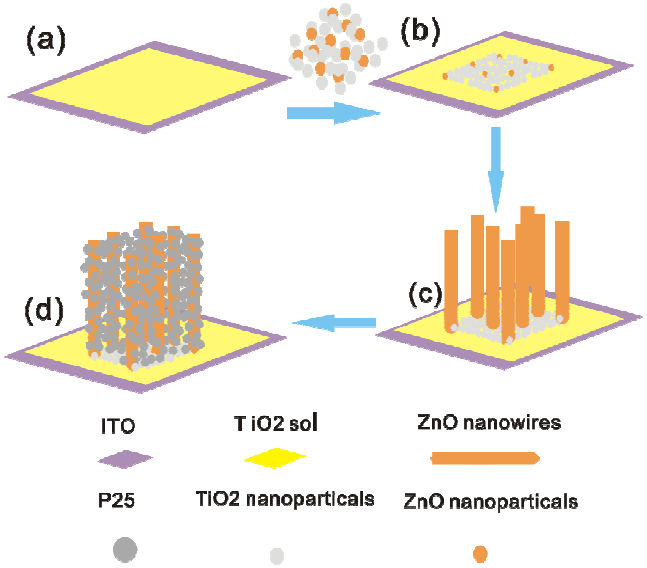

Figure1. The detailed strategy for the synthesis of TiO_2 NPs/ZnO NWs hybrid photoelectrode.

The detailed strategy of synthesizing TiO_2 NPs/ ZnO NWs hybrid photoelectrode is illustrated in Fig.1. The TiO_2 sol, serving as glue to provide a strong interaction between NPs and the substrate, was first spin-coated on ITO substrate, as we can see from Fig.1a. After the spin-coating of TiO_2 sol, immediately, the TiO_2 NPs/ ZnO NPs hybrid colloids were spin-coated (2000rpm, 30s, once) (Fig.1b). We already used ZnO NPs sol alone to prepare seed films, and the density of NWs decreased by decreasing

the concentration of ZnO NPs. The findings were that the island-like NWs film arose (very dense or very sparse in some location) when the concentration was below 5 mg/ml, and the NWs were still very dense when the concentration was over 5mg/ml (see Fig.S1, Supplementary Information). In this paper, ZnO NPs were spaced by TiO_2 NPs, the density of ZnO NWs was regulated by the ratio of ZnO NPs to TiO_2 NPs and the concentration of ZnO NPs. Then the wet films were annealed at 450°C for 0.5h in air and ZnO seed films were obtained.

Fig.1c shows the growth of the ZnO NWs, which was performed in procedure similar to that in our previous paper [7]. In the previous experiment ZnO seeds were not regulated, so the NWs easily fused when longer. Herein, the purpose of introducing TiO_2 NPs was to space ZnO NPs, ZnO NWs only grown in the position where ZnO NPs seed. Density-controlled synthesis of ZnO NWs was completed at certain ratio of ZnO/TiO_2 and concentration of ZnO NPs. Another precondition of filling paste is the preparation of TiO_2 paste with good fluidity. TiO_2 paste was accomplished by reference literature [13]. It was difficult to fill paste in the gap among NWs by printing pressure and own gravity, so the samples were stuck on inwall of the centrifuge and the paste was filled by larger centrifugal force (5000 r/min, 10 min) after the paste was coved on ZnO arrays by screen printing as shown in Fig. 1d. After the process from printing to filling was repeated 2 cycles, the samples were annealed at 450°C for 0.5h in air, thus the hybrid photoelectrods were obtained.

QDSSCs fabrication and physical characterization

The deposition of CdSe QDs was achieved by the successive ion layer adsorption and reaction (SILAR) method [14, 15]. 40ml of 30mM SeO_2 water solution was reduced with KBH_4 as Se^{2-} source in Ar atmosphere. Meanwhile, preparing 40ml of $Cd(NO_3)_2$ solution (30mM) as Cd^{2+} source. The SILAR process was repeated for 12 cycles.

A 60μm-thick hot-melt ionomer film (Surlyn) under heating (120°C) was then sandwiched between the sensitized photoanode and a 100nm thick Pt counter electrode. A polysulfide electrolyte of 0.5M Na_2S, 2M S, and 0.2M KCl in a methanol/water (7:3 by volume) was injected via the predrilled hole of Pt.

The crystalline phase of photoelectrods were identified by the X-ray diffraction (XRD) using a D/max-2400 X-ray diffraction spectrometer (Rigaku) with Cu Ka radiation and operated at 40kV and 100mA from 20 to 70^o, and the scanning speed was 15^o min−1 at a step of 0.02^o. The morphologies of the samples were analyzed using a field emission scanning electron microscopy (FESEM, HITACHI S-4800). The transmittance spectra and absorption spectra of films were recorded at 300-800nm with a JascoV-570 UV-Vis-NIR photospectroscometer. The I-V characteristics were tested under 100mW/cm^2 AM 1.5G simulated sunlight (100W Xe source). I(V) were recorded by a Keithley 2400 source meter (active area is 0.25cm^2). It should be noted that the solar simulator was previously calibrated by using a Si reference cell equipped with a KG-5 filter. The external quantum efficiency (EQE) system uses a lock-in amplifier (SolarCellScan 100, Zolix, China) to record the short circuit currents under chopped monochromatic light.

Results and discussion

SEM analysis

In this paper, there are two challenges that we must settle in preparation of this novel hybrid structure, one is the density-controlled synthesis of ZnO NWs, and another is the injection of TiO_2 paste. The former one is more difficult to handle. The paste can be well injected only when the gap among the NWs is large enough. The gap is dominated by the density of NWs, eventually regulated by the amount of ZnO NPs that were spin-coated on the ITO substrate. Finally, we regulated the density of NWs by the ratio of ZnO NPs to TiO_2 NPs and the concentration of ZnO NPs. The results are shown in Fig.2. Fig.2(a-c) shows the cross-section SEM of NWs synthesized using the different ratio of hybrid colloids (22.5:2.5, 11.5:11.5 and 2.5:22.5) as seeds precursor. It can be seen that the density of NWs decreased as the radio decreased, but this is not obvious. With the low ratio of 2.5:22.5, the density of NWs is still high which can be seen in Fig.2c. It is possible that the concentration of ZnO NPs is still high and the density of seeds exploitable for the NW growth is similar for the three

samples although the ratio of 2.5:22.5 is low. (i.e. the lower ZnO:TiO_2 ratio should allow to higher density). The NWs are in a mess or not observed on substrates when the ratio (ZnO:TiO_2) is lower than 2.5:22.5 (e.g.1.25:23.75,0.25:24.75), so we regulate the density of NWs by decreasing the concentration of ZnO NPs under the ratio of 2.5:22.5. Fig.2(c-f) shows the cross-section SEM of NWs grown on seeds prepared by 2.5, 0.625, 0.156 and 0.039mg/ml ZnO NPs hybrid colloid, respectively. It can be seen that the density of NWs obviously decreased with the decrease of the concentration of ZnO NPs. The gap was large enough for TiO_2 paste to inject when the concentration was below 0.1mg/ml. As we can see from the above, compared with ratio, concentration plays a more important role in determining the density of NWs. Previously the authors used pure ZnO NPs as seeds precursor to synthetize NWs. Experimental results show the seed films were poor when the concentration of pure ZnO NPs was below 5mg/ml. Thus, in this experiment TiO_2 plays two roles, it not only helps to regulate the density of NWs, but also contributes to lower the concentration of ZnO NPs.

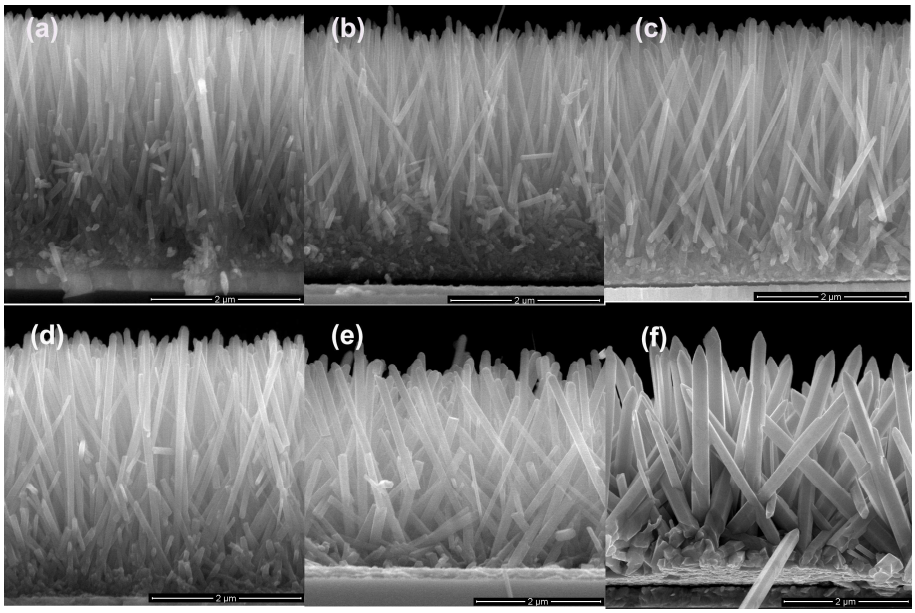

Figure2. The cross-section SEM of NWs synthesized using the different ratio of ZnO NPs to TiO_2 NPs (a-22.5:2.5, b-11.5:11.5 and c-2.5:22.5 (mg/ml:mg/ml)) as seeds precursor, and the different concentration of ZnO NPs (d-0.625, e-0.156 and f-0.039 mg/ml) as seeds precursor under 2.5:22.5, respectively.

ZnO NWs were synthesized by chemical bath deposition (CBD) method [6], the seed films were immersed in a 100ml mixed aqueous solution of 0.04M $Zn(NO_3)_2$ and 0.8M NaOH at 80 °C for 1 h. The length of NWs varied in the range of 3.27-3.44μm and the difference is not significant as we can see from Fig.2. With the decrease of ratio from 22.5:2.5, 11.5:11.5 to 2.5:22.5, the diameter of NWs changes from 130, 150 to170nm, indicating an unconspicuous change. Nevertheless, with the decrease of concentration of ZnO NPs from 0.625, 0.156 to 0.039mg/ml, the diameter of NWs increased obviously from 180, 220 to 380nm. There are different explanations for the phenomenon .

Lee et.al thought the growth of ZnO microrods could be considered as a two-stage growth: the growth process of ZnO rods, which bundle together, and the growth steps via the coalescence mode. Therefore, the bundle of ZnO nanorods could be further transformed to microrods [16]. Guo et.al proposed two density-dependent growth regimes: independent growth regime, where the spacing between adjacent NWs is larger than 2λs (the diffusion length of Zn adatoms on substrate surface), and competitive growth regime where NWs compete for Zn adatoms due to overlapped surface collection areas [17]. Kang et.al thought the low density ZnO NWs grown at the edge of patterned seeds have larger diameters because of a greater precursor chemical source supply than is present for the high density ZnO NW s in the central regions of patterned seeds [18]. We think this can been better explained using the comprehensive view of Guo and Wook, low density NWs (the independent growth regimes) have a greater precursor chemical source supply comparing with high density NWs (the competitive growth regimes), single NW obtains more $Zn(OH)_4^{2-}$ complex for the radial growth of the NW during unit time. When NWs are the competitive growth regimes, small gap decrease growth solution around NW, and individual NW gets less $Zn(OH)_4^{2-}$ complex for radial growth.

Mechanism analysis

In this way, the presence of ZnO NWs played two major roles, i.e., promoting the electron transfer and increasing the light scattering. Fig.3(a, b) illustrates different

electron diffusion processes in a bare TiO_2 NPs and the obtained TiO_2 NPs/ZnO NWs hybrid films, respectively. In bare TiO_2 NPs film, electrons transport via a zigzag pathway through the NPs and a large number of grain boundaries result in the increment of charge recombination. In the TiO_2 NPs/ZnO NWs hybrid film, these NWs supply the highway within TiO_2 NP, the generated electrons breadthwise diffuse to ZnO NWs through a small quantity of grain boundaries of TiO_2 NPs and length -ways transport to ITO by one-way. In addition, Fig.3(a, b) also illustrates sunlight transmission processes in a bare TiO_2 NPs and the obtained TiO_2 NPs/ZnO NWs hybrid films, respectively. In bare TiO_2 NPs film, sunlight transmission linearly and there is not light scattering, and some light transmit out of the film and waste. In the TiO_2 NPs/ZnO NWs hybrid film, these NWs supply the scattering centers of light and the opticalpath was increased by the multiple reflection, so the sunlight was sufficiently absorbed.

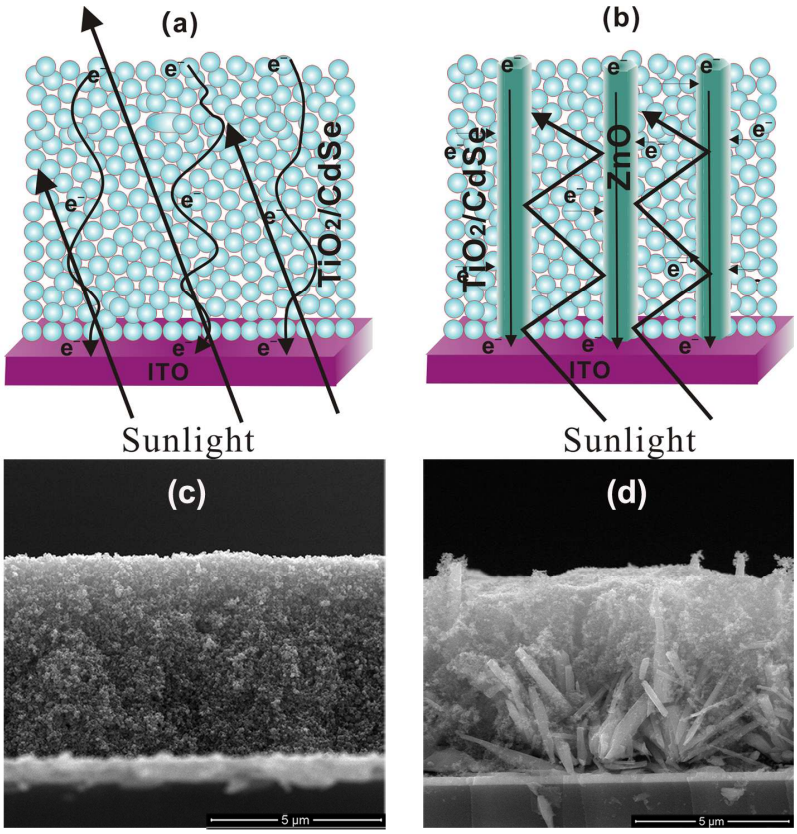

Figure3.Schematic illustration of electron (e−) diffuse transport and light transmission within the NPs film (a) and NPs/NWs film (b). Cross-section SEM images of (c) bare

TiO_2 NPs and (d) TiO_2 NPs /ZnO /NWs hybrid films. (Blue sphere, red shell, and green pillar represent TiO_2 NPs, CdSe QDs, and ZnO NWs, respectively.)

The density of ZnO NWs was controlled in 3.1 section, in addition, the injection of TiO_2 paste is also a crucial step. Fig.3(c, d) shows cross SEM of the bare TiO_2 NPs film and TiO_2 NPs/ZnO NWs hybrid film. The bare TiO_2 NPs film was porous and homogeneous in Fig.3c. From Fig.3d TiO_2 paste was successfully injected into the gap among ZnO NWs, but it did not completely reach the bottom. Big gap existed due to the tilt of NWs, which was detrimental to the cell. We will improve verticality of NWs in subsequent work.

XRD and optic characteristic of films

Fig.4a shows XRD patterns of the TiO_2 NPs/ ZnO NWs hybrid film and pure ZnO NWs film prepared on ITO substrates. As indicated in the XRD patterns, all diffraction peaks of the hybrid film and the pure ZnO NWs film can be well indexed to hexagonal wurzite ZnO (JCPDS No. 36-1451) and anatase TiO_2 (JCPDS No. 21-1272). Apparently, after injecting TiO_2 paste, the intensities of all ZnO peaks decreased due to the coverage of TiO_2.

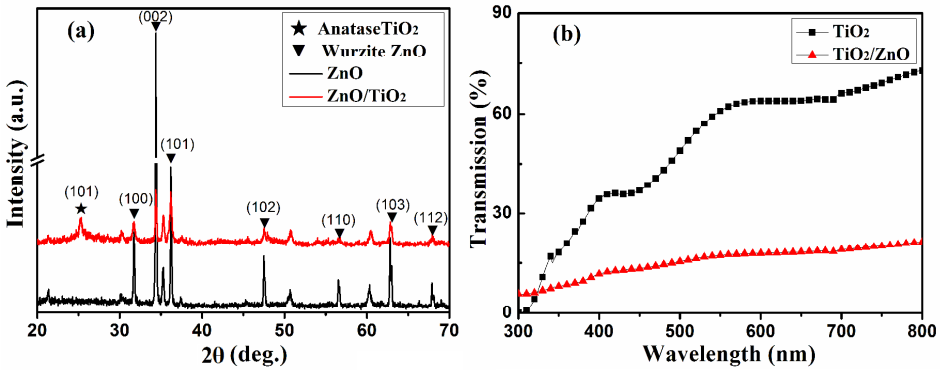

Figure4. (a) XRD patterns of ZnO NWs and TiO_2 NPs/ZnO NWs films on ITO substrates; (b) Transmittance spectra of TiO_2 NPs and TiO_2 NPs/ZnO NWs films without CdSe.

The transmissivity of the films was studied to investigate the scattering effect of the ZnO NWs. Fig.4b shows the transmittance spectra of TiO_2 NPs/ZnO NWs hybrid film and TiO_2 NPs film without CdSe, the films have similar thickness. Apparently, the

hybrid film had lower transmissivity (< 20%) in the visible wavelength range of 400-800nm than that (> 36%) of bare TiO_2 NPs film, suggesting the combination of ZnO NWs and TiO_2 NPs led to the higher light harvesting efficiency and most of the light was restricted within the photoanodes. This evidence confirmed the light scattering effect of the ZnO NWs in the TiO_2 NPs film.

Performance of cells

Introducing ZnO NWs into TiO_2 NP films greatly reduces the transmission of light (Fig4b), which indicates ZnO NWs has high scatting effect to injected light. The scattering promote the increase of absorption spectra and photon-to-electron conversion efficiency. Fig.5(a-c) shows the absorption spectra of cells in the visible light, EQE and I-V curve of cells.

UV-vis absorption spectra in Fig.5a shows the absorption intensity and absorption onset as increasing the cycle times of depositing CdSe. The absorption onset has a red shift from 650nm to 750nm with the deposition times from 6 to 12 and the absorption intensities are same. TiO_2/CdSe, ZnO/CdSe and TiO_2/ZnO/CdSe have the same absorption onset of 750nm when the circle is 12 times. But the absorption intensities of ZnO/CdSe and TiO_2/ZnO /CdSe in the wavelength range of 350nm-650nm are higher than that of TiO_2/CdSe due to the scatting effect of ZnO NWs. The absorption spectra of TiO_2/ZnO/CdSe is similar to ZnO/CdSe. The specific surface area of 1D nanostructure films is roughly an order of magnitude lower than that of NP films when they have a same thickness, as was mentioned in the introduction, so the adsorption of sensitizer is relatively low and the light absorption is also weak. But, here the absorption of ZnO NW films has enhanced, we think the key reason is that the light scattering effect of NWs is very good and injected light is fully absorbed after multiple reflection. From the analysis of absorption spectra, 1D nanostructure can improve light absorption of cells via the scatting effect.

Using TiO_2/CdSe，ZnO/CdSe and TiO_2/ZnO/CdSe, we fabricated solar cells to evaluate their PV performances. The I–V characteristics for QDSSCs were measured at an illumination of one sun in Fig.5b. In order to obtain a better understanding on

the effect of the amount of CdSe and the structure of photoanodes on the PV performance, table1 summarizes the open-circuit voltage (Voc), short-circuit current density (Jsc), fill factor (FF), and η of cells. Firstly, we investigated the effect of cycle times of depositing CdSe on the efficiency of cells using bareTiO_2 NPs film as photoanode. From Fig.5b and table1, the Voc, Jsc, FF, and η increased with the increase of depositing CdSe. The Voc in electrochemical QDSSCs corresponds to the difference of the quasi-Fermi level of the semiconductor E_{fn} with respect to the dark value (E_{f0}), which equals the electrolyte redox energy ($E_{f0}=E_{redox}$). Therefore, it can be written as Equation:

$$Voc=(E_{fn}-E_{f0})/e =(K_BT/e)\ln(n/n_0) \qquad \text{Eq. (A.1)}$$

where K_BT, e, n_0 are the thermal energy, the positive elementary charge, and the concentration in the dark, respectively [19, 20]. The adsorption of QDs increased with the increase of deposition times, which helped to produce more photons under the same testing conditions, more electrons were obtained by capturing more photons and transferred to the conduction band (CB) of the semiconductor. This induced the shift of the Fermi level into the CB and the increase of Voc. Meanwhile, more photo -generated carriers transported in external circuit and Jsc increased from 2, 2.91 to 5.1 mA/cm^2. From table1, FF increased from 52.3%, 53.9% to 59.1%, the reason is that QDs were more dense on the surface of TiO_2 with the increase of deposition time, which reduced the contact between electrolyte and TiO_2 arousing the recombination of carriers. The photovoltaic conversion efficiency of QDSSCs was estimated, the η improved from 0.41, 0.67 to 1.3% with the increase of CdSe due to the increase of Jsc, Voc and FF. Secondly, we carry out the comparison of TiO_2/CdSe, ZnO/CdSe TiO_2/ZnO/CdSe cells, and the best efficiencies were shown in Fig. 5b and table1. The films of TiO_2, ZnO and TiO_2/ZnO have same thickness. It was seen that ZnO/CdSe cell has a high Voc of 0.61V and TiO_2/CdSe cell has a low Voc of 0.43V. The difference of Voc between them was due to the electron mobility of optical electrode materials. The electron mobility of ZnO is higher than that of TiO_2, which lead to rapid transfer of photoelectrons to the CB. And the high electron concentration in CB induced the shift of the Fermi level into the CB and led to a larger energy band gap, so

the Voc increased [10]. TiO_2/CdSe cell has a high Jsc due to the large specific surface area, however, comparing with TiO_2/CdSe cell, TiO_2/ZnO /CdSe cell has a improvement in Voc owing to the introduction of ZnO NWs. Here, there are two important factors affecting current density, one is that the large specific surface area can increase the adsorption of the sensitizer and improve the light absorption, the other is that the scattering effect of ZnO NWs improve the effective use of light. So the large specific surface area of TiO_2 NPs and the light scatting of ZnO NWs fully improved the Jsc of TiO_2/ZnO/CdSe cell. In addition, ZnO NWs supplied the highway for photon-generated electrons and accelerated the electron collection. However, it is also seen that the FF of TiO_2/CdSe cell is the highest, whether ZnO materail effects the FF remained unclear and further investigations will be carry out in future works. Overall, TiO_2/ZnO/CdSe cell yielded the 19.2% and 30.3% enhancements in power conversion efficiency (1.55%) over optimized TiO_2/CdSe cell and ZnO/CdSe cells.

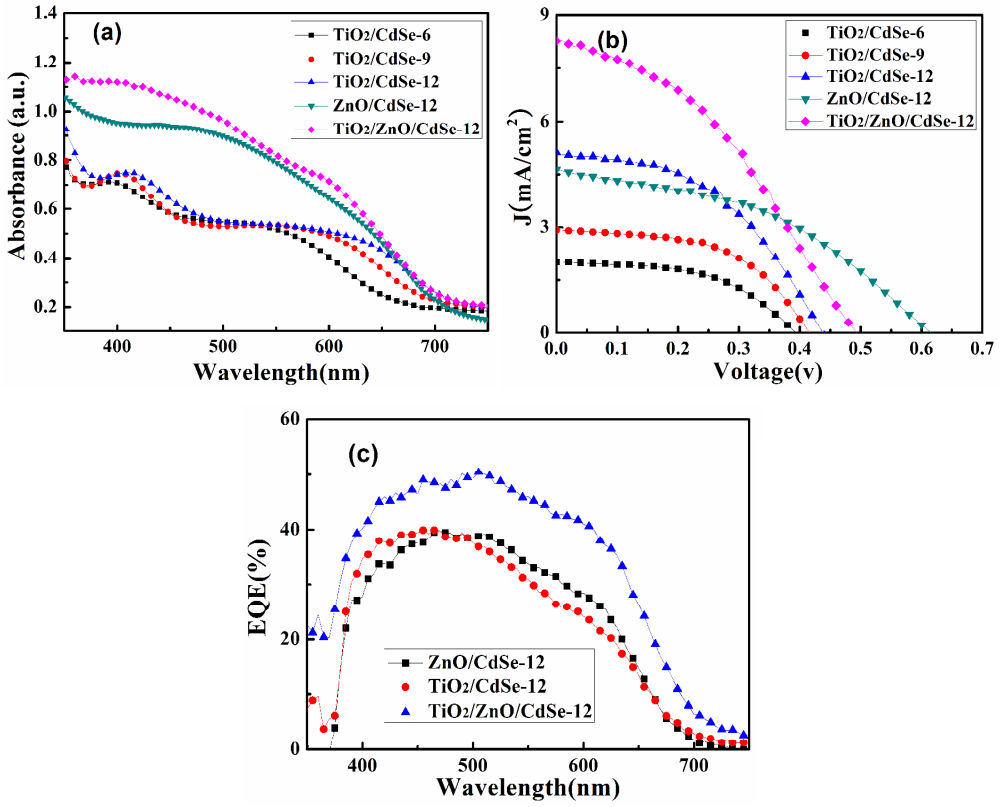

Fig. 5 (a) UV-vis absorption spectra,(b) photocurrent–voltage curves and (c) external quantum efficiency (EQE) of ZnO/CdSe, TiO_2/CdSe and TiO_2/ZnO/CdSe solar cells. (6, 9 and 12 are cycle times of depositing CdSe)

Table1. Photovoltaic parameters obtained from the I–V curves using TiO_2/CdSe, ZnO/CdSe and TiO_2/ZnO/CdSe cells.

Cells	Voc (v)	J(mA/cm^2)	FF(%)	η(%)
TiO_2/CdSe-6	0.39	2.00	52.3	0.41
TiO_2/CdSe-9	0.41	2.92	53.9	0.67
TiO_2/CdSe-12	0.43	5.10	59.1	1.30
ZnO/CdSe-12	0.61	4.64	42.3	1.19
TiO_2/ZnO/CdSe-12	0.48	7.90	40.9	1.55

Fig.5c shows the external quantum efficiency (EQE) spectra of representative CdSe sensitized solar cells based on different photoanodes. In general, the EQE for wavelengths close to the quantum dots absorption edge is relatively lower than for short wavelengths. This is mainly due to the optical losses (i.e. lower absorptance for wavelengths close to the absorption onset, Fig.5a). Strong enhancement of EQE is observed when ZnO NWs were introduced TiO_2 NPs films. And because ZnO NWs improved the scatting of longer wavelength, further improvement at longer wavelength (500-600nm) is realized. It also was shown that the EQE of ZnO NWs cell is higher than that of TiO_2 NPs cell in range of 500-600nm. The increased photocurrent and EQE are likely to be related to the change of absorption characteristics

Conclusion

In conclusions, we have reported the fabrication and characterization of the TiO_2 NPs/ ZnO NWs hybrid photoanode-based CdSe-sensitized solar cell. SEM image of ZnO NWs shows a density controlled synthesis of ZnO NWs. The density of NWs was controlled by regulating the ratio of ZnO NPs to TiO_2 NPs and the concentration of ZnO NPs in hybrid seeds precursor. The gap was large enough for TiO_2 paste to fill when the ratio of ZnO NPs to TiO_2 NPs and concentration of ZnO NPs were 1:9 and below 1mg/ml. The hybrid photoanode had low transmission, high absorption and EQE in the visible wavelength of 400-800 nm than bare TiO_2 NPs film, suggesting the combination of ZnO NWs and TiO_2 NPs led to the higher light harvesting efficiency

of the photoanode. CdSe QDSSCs based on TiO_2 NPs film, ZnO NWs film and TiO_2 NPs / ZnO NWs hybrid film were fabricated, J-V curves exhibit a marked enhanced Jsc of 7.9 mA/cm^2 and η of 1.55% for TiO_2/ZnO cell, this η has a 19.2% and 30.3% enhancements as compared to the TiO_2 NPs device with η of 1.3% and ZnO NWs device with η of 1.19%.

Acknowledgments

This work has been partially supported by the NSFC Major Research Plan on Nanomanufacturing (Grant No. 91323303). The authors gratefully acknowledge financial support from Natural Science Foundation of China (Grant Nos. 61176056 and 91123019), 111 program (No. B14040) and the open projects from Institute of Photonics and Photo-Technology, Provincial Key Laboratory of Photoelectronic Technology, Northwest University, China.

References

[1] Z.H. Lin, M.Q. Wang, L.Y. Zhang, Y.H. Xue, X. Yao and H.W. Cheng, J.T. Bai, *J. Mater. Chem.*, 2012, 22, 9082.

[2] Z. Yang, M.Q. Wang, Y.H. Shi, X.H. Song, Z.H. Lin, Z.Y. Ren and J.T. Bai, *J. Mater. Chem.*, 2012, 22, 21009.

[3] J.D. Fan, Y. Hao, A. Cabot, E. M. J. Johansson, G. Boschloo and A. Hagfeldt, *ACS Appl. Mater. Interfaces*, 2013, 5, 1902.

[4] Z. Yang, C-Y. Chen, C-W. Liu, C-L. Li and H-T. Chang, *Adv. Energy Mater.*, 2011, 1, 259.

[5] Y. Bai, H. Yu, Z. Li, R. Amal, G.Q. Lu and L.Z. Wang, *Adv. Mater.*, 2012, 24, 5850.

[6] S.Wooh, H.Yoon, J-H. Jung, Y-G. Lee, J.H. Koh, B. Lee, Y. S. Kang and K. Char, *Adv. Mater.*, 2013, 25, 3111.

[7] J.P. Deng, M.Q. Wang, X.H. Song, Y.H. Shi and X.Y. Zhang, *J. Colloid Interface Sci.*, 2012, 388, 118.

[8] M.D. Ye, D.J. Zheng, M.Q. Lv, C. Chen, C.J. Lin and Z.Q. Lin, *Adv. Mater.*, 2013, 25, 3039.

[9] L. Forro, O. Chauvet, D. Emin, L. Zuppiroli, H. Berger and F. Levy, *J. Appl. Phys.*, 1994, 75, 633.

[10] J.P. Deng, M.Q. Wang, J. Liu and X.H. Song, *J. Colloid Interface Sci.*, 2014, 418, 277.

[11] K. Zhu, N. R. Neale, A. Miedaner and A. J. Frank, *Nano. Lett.*, 2007, 7, 69.

[12] M. Seol, H. Kim, Y. Tak and K. Yong, *Chem. Commun.*, 2010, 46, 5521.

[13] X.H. Song, M.Q. Wang, J.P. Deng, Z. Yang, C.X. Ran, X.Y. Zhang and X. Yao, *ACS Appl. Mater. Interfaces*, 2013, 5, 5139.

[14] J.P. Deng, M.Q. Wang, X.H. Song and J. Liu, J. Alloys Compd., 2014, 588, 399.

[15] H.J. Lee, M.K. Wang, P. Chen, D.R. Gamelin, S.M. Zakeeruddin, M. Grätzel and M.K. Nazeeruddin, *Nano. Lett.*, 2009, 9, 4221.

[16] J-H Lee, M-H. Hon, Y-W. Chung and I-C. Leu, *J. Am. Ceram. Soc.*, 2009, 92, 2192.

[17] D. L. Guo, L. H. Tan, Z. P. Wei, H.Y. Chen and T. Wu, *Small*, 2013, 9, 2069.

[18] H. W. Kang, J. Yeo, J.O. Hwang, S. Hong, P. Lee, S.Y Han, J. H. Lee，Y. S. Rho, S. O. Kim, S. H. Ko and H. J. Sung, *J. Phys. Chem. C,* 2011, 115, 11435.

[19] A. Zaban, M. Greenshtein and J. Bisquert, *Chemphyschem*, 2003, 4, 860.

[20] J. Bisquert, A. Zaban and P. Salvador, *J. Phys. Chem. B*, 2002, 106, 8774.

Captions

Figure1. The detailed strategy of the synthesis of the TiO_2 NPs/ZnO NWs hybrid photoelectrode.

Figure2. The cross-section SEM of NWs synthesized using the different ratio of ZnO NPs to TiO_2 NPs (a-22.5:2.5, b-11.5:11.5 and c-2.5:22.5 (mg/ml:mg/ml)) as seeds precursor, and the different concentration of ZnO NPs (d-0.625, e-0.156 and f-0.039 mg/ml) as seeds precursor under 2.5:22.5, respectively.

Figure3. Schematic illustration of electron (e−) diffuse transport in (a) the NPs and (b) NPs/NWs hybrid films. Cross-section SEM images of (c) bare TiO_2 NPs and (d) TiO_2 NPs/ZnO NWs hybrid electrode. (Blue sphere, red shell, and green pillar represent TiO_2 nanopartical, CdSe quantum dot, and ZnO nanowire, respectively.)

Figure4. (a) XRD patterns of ZnO NPs and TiO_2 NPs/ZnO NWs hybrid film on ITO substrates; (b) Transmittance spectra of bare TiO_2 NP film and TiO_2 NPs/ZnO NWs hybrid film with the similar thickness.

Fig.5(a) UV-vis absorption spectra,(b) photocurrent–voltage (I–V) curves and (c) external quantum efficiency (EQE) of ZnO/CdSe, TiO_2/CdSe and TiO_2/ZnO/CdSe solar cells. (6, 9 and 12 are cycle times of depositing CdSe)

Table1. Photovoltaic parameters obtained from the I–V curves using TiO_2/CdSe, ZnO/CdSe and TiO_2/ZnO/CdSe cells.